

## Energy Sources, Part A: Recovery, Utilization, and Environmental Effects

ISSN: 1556-7036 (Print) 1556-7230 (Online) Journal homepage: <http://www.tandfonline.com/loi/ueso20>

# Two-dimensional numerical modeling of combustion of Jordanian oil shale

Jamil J. Al Asfar, Ahmad Hammad, Ahmad Sakhrieh & Mohammad A. Hamdan

**To cite this article:** Jamil J. Al Asfar, Ahmad Hammad, Ahmad Sakhrieh & Mohammad A. Hamdan (2016) Two-dimensional numerical modeling of combustion of Jordanian oil shale, Energy Sources, Part A: Recovery, Utilization, and Environmental Effects, 38:9, 1189-1196, DOI: 10.1080/15567036.2014.880091

**To link to this article:** <http://dx.doi.org/10.1080/15567036.2014.880091>



Published online: 09 May 2016.



Submit your article to this journal [↗](#)



Article views: 5



View related articles [↗](#)



View Crossmark data [↗](#)

## Two-dimensional numerical modeling of combustion of Jordanian oil shale

Jamil J. Al Asfar<sup>a</sup>, Ahmad Hammad<sup>a</sup>, Ahmad Sakhrieh<sup>a,b</sup>, and Mohammad A. Hamdan<sup>a</sup>

<sup>a</sup>Mechanical Engineering Department, The University of Jordan, Amman, Jordan; <sup>b</sup>Department of Mechanical and Industrial Engineering, American University of Ras Al Khaimah, Ras Al Khaimah, UAE

### ABSTRACT

A two-dimensional (2-D) modeling of the burning process of Jordanian oil shale in a circulating fluidized bed (CFB) burner was done in this study. The governing equations of continuity, momentum, energy, mass diffusion, and chemical combustion reactions kinetics were solved numerically using the finite volume method. The numerical solution was carried out using a high-resolution 2-D mesh to account for the solid and gaseous phases,  $k-\epsilon$  turbulence, non-premixed combustion, and reacting CFD model with the same dimensions and materials of the experimental combustion burner used in this work. The temperature distribution and evolution of species were also computed.

Proximate and ultimate analyses were also performed to evaluate the air–fuel ratio and ash content. The required thermophysical properties, such as heating value, density, and porosity were obtained experimentally, while the activation energy was obtained from published literature.

It was found that the temperature contours of the combustion process showed that the adiabatic flame temperature was 1080 K in a vertical burner, while the obtained experimental results of maximum temperature at various locations of the burner in actual, non-adiabatic, non-stoichiometric combustion reached 950 K, showing good agreement with the model.

### KEYWORDS

2-D combustion model; adiabatic flame temperature; direct burning; oil shale; ultimate and proximate analysis

## 1. Introduction

The utilization of oil shale is achieved by several techniques, such as direct burning or extraction of oil in a liquid form from solid oil shale through pyrolysis or solvent extraction at sub- and super-critical conditions. Direct combustion involves generation of heat by direct combustion of oil shale. A circulated fluidized bed is used to enhance the efficiency and reduce the emission of harmful gases. This technique is applied in many countries and the results are encouraging (Jaber and Probert, 1999).

During combustion, oil shale undergoes the stages of ignition, devolatilization, and solid char particle combustion. Ignition is considered as the process initiating the combustion phenomenon. It is very important due to its influence on flame stability, pollutant formation and emission, and flame extinction. Devolatilization involves the emission of volatile gaseous matter, which is ignited and undergoes homogenous combustion after heating a specific temperature. Solid char particle combustion, ignited as a result of volatile combustion followed by a heterogeneous reaction, involves the direct attack by oxygen on solid particles (Jaber and Probert, 1999; Turns, 2000).

**CONTACT** Jamil J. Al Asfar ✉ [jamilasfar@yahoo.com](mailto:jamilasfar@yahoo.com); [jasfar@ju.edu.jo](mailto:jasfar@ju.edu.jo)  Mechanical Engineering Department, The University of Jordan, P. O. Box 2583, Amman 11181, Jordan.

Color versions of one or more of the figures in the article can be found online at [www.tandfonline.com/ueso](http://www.tandfonline.com/ueso).

© 2016 Taylor & Francis Group, LLC

Combustion of oil shale can produce significant amounts of pollutants, such as sulfur dioxide ( $\text{SO}_2$ ) and  $\text{NO}_x$  that result in acid rain and photochemical smog. The concentration of  $\text{SO}_2$  increases with bed temperature when first reaching its maximum value at  $750^\circ\text{C}$ . But, above  $750^\circ\text{C}$ , it decreases with increased bed temperature. It also decreases with increasing circulating ratio, while it increases with increase of secondary air ratio. The concentrations of  $\text{NO}$  and  $\text{NO}_2$  increase with bed temperature when first reaching a maximum at  $850^\circ\text{C}$ , and above  $850^\circ\text{C}$  these decrease with increased bed temperature. Also,  $\text{NO}$  and  $\text{NO}_2$  concentrations decrease with secondary air ratio.  $\text{N}_2\text{O}$  concentration reduces with increasing bed temperature while it increases with secondary air ratio. In general, ash is an inorganic byproduct of the combustion of oil shale, and it causes environmental problems with consequent attempts made to benefit from such materials, especially in the construction industry (Jaber and Probert, 1999; Turns, 2000; Behjat et al., 2008).

Behjat et al. (2008) investigated hydrodynamic and heat transfer phenomena in a gas-solid fluidized bed reactor by simulation using the computational fluid dynamic (CFD) technique. The governing equations and boundary conditions were introduced then solved using a computer program. The results were compared to reported experimental data to validate the model, and showed good prediction of hydrodynamic behavior. The results showed that gas temperature increases as it rises in the reactor due to heat from the polymerization reaction, leading to higher temperatures at the top of the bed.

Gungor (2009) developed a one-dimensional model for a char circulating fluidized bed (CFB) involving volatilization, attrition, and combustion. The analyses focused on two regions: a bottom zone considered as a bubbling fluidized bed, and an upper zone where a core annulus solids flow structure was established. The effect of operational parameters – particle diameter, superficial velocity, and air–fuel ratio – was studied using this model. The results were then compared to test results obtained from a 50 kW unit and good agreement was obtained.

Jordan is a country rich in oil shale resources, estimated to exceed 50 billion tons, with an oil content of around 4 billion tons (Ministry of Energy and Mineral Resources of Jordan, 1994). Jordanian oil shale is of a good quality with high organic matter content, suitability for surface mining, and is well located in regard to potential consumers. These factors encourage the utilization of Jordanian oil shale, which has been successfully processed in CFB (Russel, 1990; Ministry of Energy and Mineral Resources of Jordan, 1994; Hamarneh, 1998). Qudah et al. (2010) performed experimental analysis to determine the proximate and ultimate analysis of Jordanian oil shale. They estimated the heating value and composition in terms of C, H, O, N, S, moisture, and ash content.

In this study, a 2-D mathematical model for the combustion process of Jordanian oil shale was carried out. This included temperature contours and selected combustion products such as  $\text{CO}$ ,  $\text{CO}_2$ , and S. The physical model consisted of an experimental combustion unit composed of a vertical combustion chamber (0.5 m diameter, 3 m height), two cyclones (0.3 m diameter), and a temperature measurement system. The 2-D mathematical model was implemented to solve numerically the governing equations of simultaneous heat and mass transfer including continuity, momentum, energy, mass diffusion, and chemical combustion reactions kinetics, using the finite volume method based on two inlets for air streams – one from the bottom (axial) and the other from the side – with the same inlet for injected fuel particles, as shown in Figures 2–4 and 6.

Those equations were solved using a high-resolution mesh accounting for the solid and gaseous phases,  $k$ - $\epsilon$  turbulence, non-premixed combustion model, and reacting CFD model, with the same dimensions and materials as the experimental combustion burner in this study. The temperature values were also recorded during actual burning of oil shale and compared to theoretical values.

## 2. Composition and thermophysical properties

The elemental composition of shale oil in terms of the molar percentages of C, H, O, N, and S components was determined experimentally. The proximate composition in terms of moisture, volatiles, fixed carbon, and ash fractions was also determined. Thermal conductivity test equipment and bomb calorimetry were used to determine thermal conductivity and heating values. The results of proximate, ultimate analysis, and Fischer assay are presented in Table 1 (Al Asfar et al., 2012).

The stoichiometric fuel–air ratio ( $F/A$ ) for complete combustion is given by:

$$(F/A)_{\text{stoich}} = \left( \frac{\dot{m}_{\text{fuel}}}{\dot{m}_{\text{air}}} \right) \quad (1)$$

This ratio is found using the values of fuel components resulting from the ultimate analysis, according to Culp (1991) and Turns (2000):

$$(F/A)_{\text{stoich.}} = \frac{0.232}{2.66C + 7.94H_2 + 0.998S - O_2} \quad (2)$$

## 3. Theoretical background

Kunii and Levenspiel defined fluidization as the operation by which solid particles are transformed into a fluid-like state through suspension in gas or liquid. The quality of fluidization is governed by factors such as size and size distribution of the solids, fluid solid density ratio, vessel geometry, and gas inlet arrangement. The minimum fluidization velocity is the point reached by the velocity of upward flowing of the fluid where the frictional force between particles and fluid exactly counterbalances the weight of the particles. This velocity, which is an important factor in the design of any fluidized bed reactor, can be found from Eq. (3) (Kunii and Levenspiel, 1991):

$$U_{mf} = \frac{d_p^2(\rho_b - \rho_f) \cdot g}{150 \cdot \mu} \cdot \frac{\epsilon^3 \cdot \phi^2}{1 - \epsilon} \quad (3)$$

where  $d_p$  is particle size,  $\rho_b$  is bulk density of the bed,  $\rho_f$  is fluid density,  $\mu$  is fluid viscosity,  $\epsilon$  is porosity, and  $\phi$  is the particle shape factor. Particle size is determined by calculating the geometrical mean of the smallest opening size of the sieve through which the particle has passed, and the largest opening size of the sieve through which the particle fails to pass. To find the relation between bulk density of the bed and the particle density, Eq. (4) is used:

**Table 1.** Ultimate (dry basis), proximate (as received), and Fischer assay analyses of raw shale samples.

Analysis, wt.%	El-Lajjun
<b>Ultimate</b>	
C	15.89
H	2.02
N	0.35
S	0.16
O	12.80
Ash	68.78
<b>Proximate</b>	
Moisture	0.72
Ash	68.78
Volatile matter	30.12
Fixed carbon	0.38
<b>Fischer assay</b>	
Shale oil	9.63
Decomposed water	1.10
Gas	2.70
Spent shale	86.57

$$\rho_b = \rho_p(1 - \varepsilon) \quad (4)$$

The mean fluidization velocity during the operation is estimated from the following correlation (Kunii and Levenspiel, 1991):

$$\frac{H}{H_{mf}} = 1 + \frac{10.978 \cdot (U_f - U_{mf})^{0.738} \cdot \rho_p^{0.376} \cdot d_p^{1.006}}{U_{mf}^{0.937} \cdot \rho_f^{0.126}} \quad (5)$$

where  $H$  is expanded bed height,  $H_{mf}$  is bed height at the minimum fluidization velocity, and  $U_f$  is fluidization velocity. Finding the terminal velocity, which is the velocity of the flow gases where the solid particles start to leave the bed, is very important in the design since it determines the energy losses in the bed and the requirement for the cyclone and recycling mechanism in regard to unburned particles. In this study, the formula of Souza and Santos for terminal velocity, which is given in Eq. (6), is used (Kunii and Levenspiel, 1991):

$$U_t = d_p \cdot \left[ \frac{4 \cdot (\rho_p - \rho_f)^2 \cdot g^2}{225 \cdot \rho_f \cdot \mu} \right]^{\frac{1}{3}} \quad (6)$$

#### 4. Mathematical model

The combustion modeling of oil shale particles of sizes 70–350  $\mu\text{m}$  is based on a non-premixed flame model of volatile material with two air inlets for air streams: one from the bottom (axial) and the other from the side, with the same inlet for injected fuel particles. The injection of solid oil shale particles is done using a screw feeder discharging them at a given mass flow rate. The model used is similar to the burner designed with the experimental fluidized bed chamber for the burning of oil shale (3 m height, 0.5 m diameter). The first air stream enters the combustion chamber from the bottom at a velocity of 2 m/s, while the fuel and second air stream enter from the left side at a fuel injection rate of 0.01 kg/s. Following this, the fuel and the two air streams will have the same vertical upward velocity.

The burner mesh, shown in Figure 1, was created using Fluent software with two velocity inlet surfaces – one for the main air stream and the other for both the fuel and the secondary air stream, a

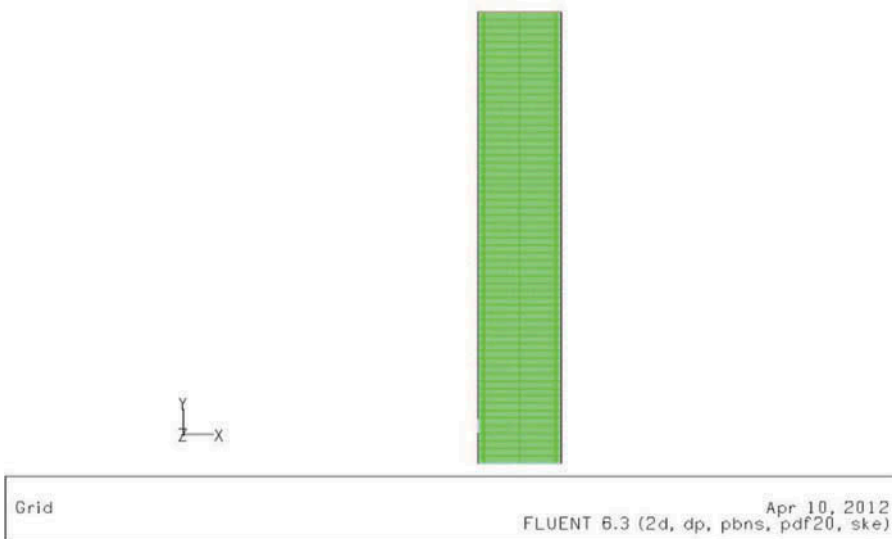


Figure 1. Fluidized bed burner mesh with two inlets – one each from the bottom and side.

pressure outlet surface at the exhaust, and three surfaces for the combustion chamber walls. Cylindrical coordinates were chosen; since the burner is cylindrical and the injection of solid particles occurs at the side inlet, as shown. Fluent solves the conservation mass and momentum (Navier–Stokes) equations for adiabatic simulations and the conservation equations of 20 chemical species. A grid independent test was performed to ensure that the mesh sizes considered produce identical results. It is also noted from the figure that the mesh size is refined at the fuel and air inlet to produce the most accurate numerical results. The energy equation considered is that according to Kunii and Levenspiel (1991) and Turns (2000):

$$\frac{\partial}{\partial t}(\rho h) + \nabla \cdot (\vec{v} \rho h) = \nabla \cdot \left( \frac{k_t}{c_p} \nabla h \right) + S_h \quad (7)$$

where the total enthalpy is defined as

$$h = \sum_j Y_j h_j \quad (8)$$

where  $Y_j$  is the mass fraction of species  $j$  and

$$h_j = \int_{T_{ref,j}}^T c_{p,j} dt + h_j^o(T_{ref,j}) \quad (9)$$

$h_j^o(T_{ref,j})$  is the formation enthalpy of species  $j$  at the reference temperature  $T_{ref,j}$ .

The mole fraction of oil shale species during the combustion process was estimated using the probability density function (PDF) module integrated in Fluent software. The reversible chemical reactions involved the following 23 chemical species: C, H, N, O, S, C(s), S(s), CH<sub>4</sub>, H<sub>2</sub>, CO, CO<sub>2</sub>, N<sub>2</sub>, O<sub>2</sub>, OH, H<sub>2</sub>O, HS, H<sub>2</sub>S, SO, SO<sub>2</sub>, CS<sub>2</sub>, NO, NO<sub>2</sub>, and C<sub>2</sub>H<sub>6</sub>.

## 5. Experimental work

Based on the equations presented in the mathematical model above, the diameter of the burner was selected to be 0.5 m, with the maximum expanded height of the bed to be twice the internal diameter. A two-cyclone system was provided in this design, the first being 0.3 m in diameter and 1 m in height, the second cyclone having the same diameter but with height 0.5 m. Figure 2 shows photographs of the cyclones and burner components. The material selected for the burner (stainless steel SX 310 S (3 mm)) was suitable for a high-temperature environment, with high temperature strength, good creep, and corrosion resistance. The air distribution plate was designed to assure good distribution of the air around the burner cross section. The diameter of the plate was 0.6 m with 3200 holes, each of 2 mm diameter and 2 apart. It was fabricated locally from the same burner material using a computerized numerical control (CNC) machine to drill the air distribution plate. Temperature measurement was accomplished using an accurate, modern, reliable real-time system through LabVIEW and 16 k-type thermocouples, installed at specific locations shown in Figure 3.

## 6. Results

The set of figures presented here show the results of direct burning of oil shale for flame temperature and CO<sub>2</sub> gas. The maximum CO<sub>2</sub> concentration reached 3.3%, as shown in Figure 6. The contours of mass CO<sub>2</sub> fraction around the combustion flame clearly show the exact flame position by noting the obvious difference in CO<sub>2</sub> concentration upstream and downstream of the flame. The temperature contours of the combustion process, presented in Figure 4, show that the adiabatic flame temperature was 1080 K, while the obtained experimental results for temperature at various locations of the burner, as seen in Figure 5, show that the maximum temperature reached 950 K, showing good agreement with our model.

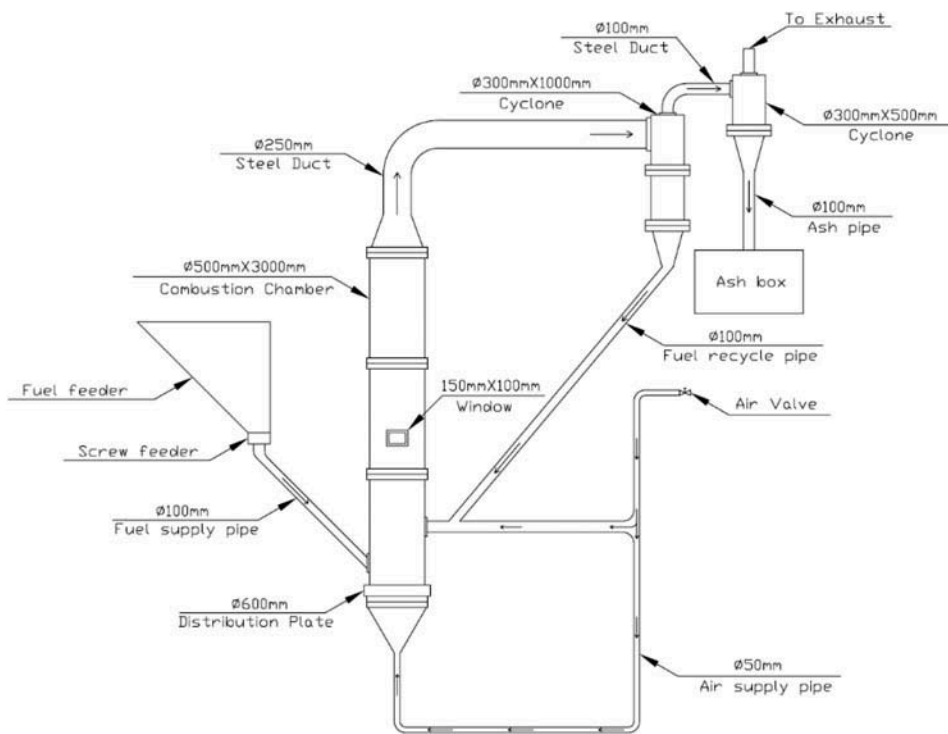


Figure 2. Circulating fluidized bed burner.

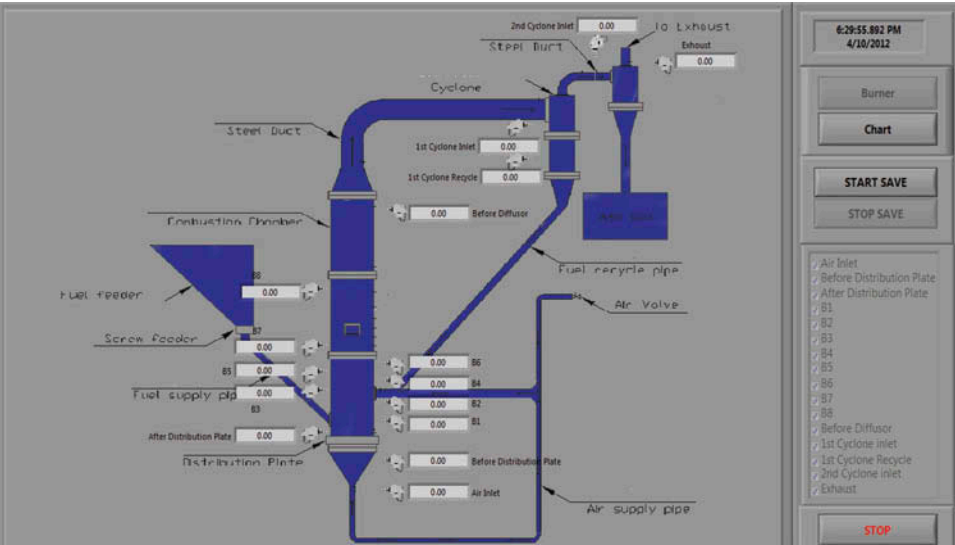


Figure 3. Screenshot for the LabVIEW interface measurement system.

The difference between experimental and theoretical results is due to the fact that the calculated theoretical temperature was based on the adiabatic flame temperature of the complete stoichiometric burning process, while the actual burning process was neither adiabatic nor stoichiometric. Also, the

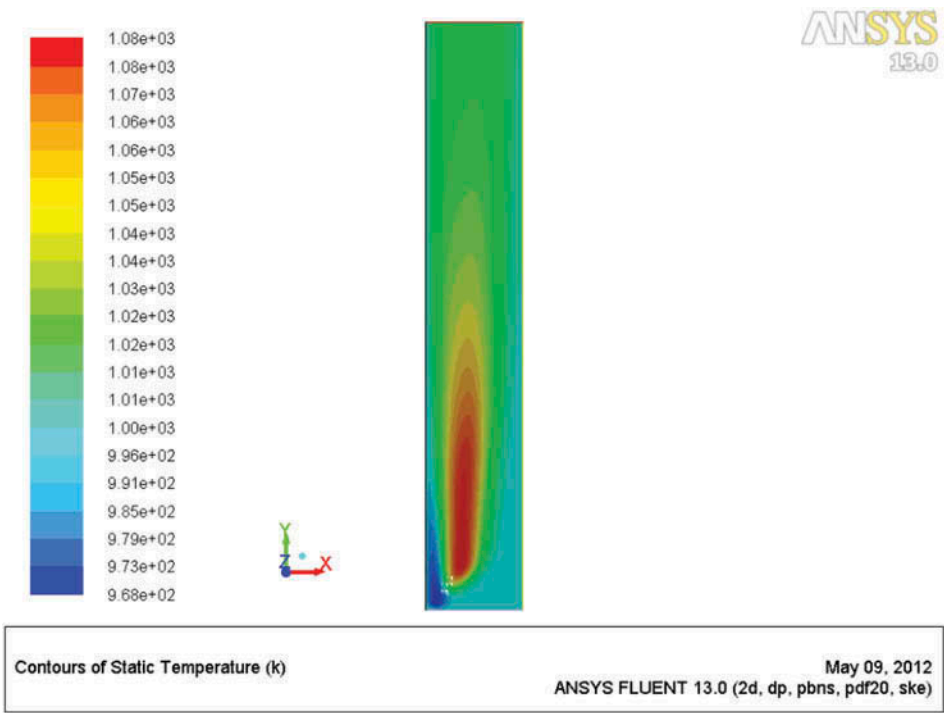


Figure 4. Temperature contours for fluidized bed oil shale combustion chamber.

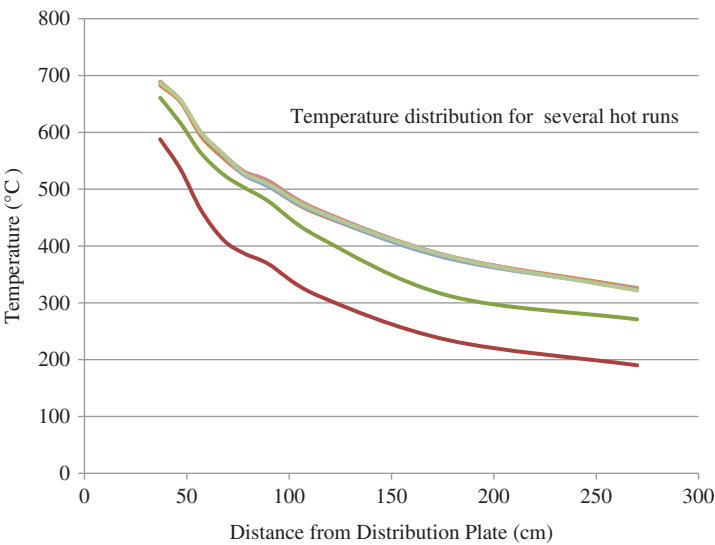


Figure 5. Temperature distribution for several hot runs of oil shale burning.



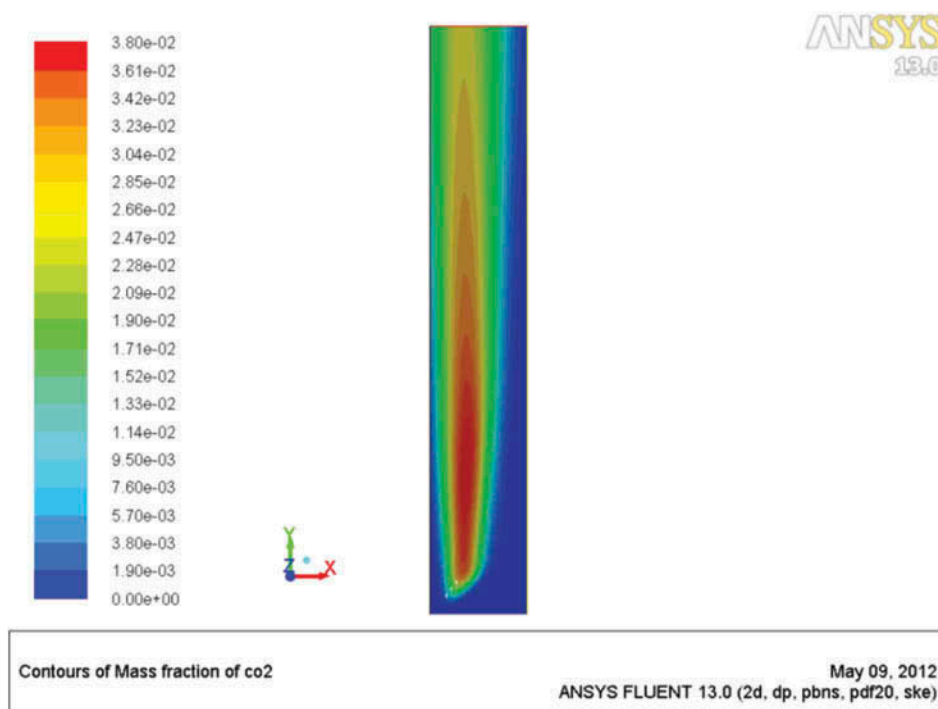


Figure 6. Mole fraction of  $\text{CO}_2$  for fluidized bed combustion chamber.

presence of a certain percentage of excess air to ensure complete combustion reduced the adiabatic flame temperature.

### Funding

The authors of this article would like to thank the Scientific Research Support Fund – Jordan for their support to this research work.

### References

- Al Asfar, J. J., Hammad, A., Sakhrieh, A., and Hamdan, M. A. 2012. Theoretical investigation of direct burning of oil shale. *12th International Combustion Symposium*, Kocaeli, Turkey, 24–26 May.
- Behjat, Y., Shahhosseini, S., and Hashemabadi, S. 2008. CFD modelling of hydrodynamic and heat transfer in fluidized bed reactors. *Int. Commun. Heat Mass Transfer* 35:357–368.
- Culp, Archie W. 1991. *Principles of Energy Conversion*, 2nd Ed. New York: McGraw-Hill.
- Gungor, A. 2009. One dimensional numerical simulation of small scale CFB combustors. *Energy Convers. Manage.* 50 (3): 711–722.
- Hamarneh, Y. 1998. *Oil Shale Resources Development in Jordan*. Amman, Jordan: Natural Resources Authority.
- Jaber, J. O., and Probert, S. D. 1999. Pyrolysis and gasification kinetics of Jordanian oil-shales. *Appl. Energy* 63(4):269–286.
- Kunii, D., and Levenspiel, O. 1991. *Fluidization Engineering*, 2nd Ed. Boston: Butterworth-Heinemann.
- Ministry of Energy and Mineral Resources of Jordan. 1994. *Annual Report*. Amman, Jordan: Ministry of Energy and Mineral Resources.
- Qudah, R., Shabbar, S., Janajreh, I., and Hamdan, M. A. 2010. Material characterization and gasification of Jordanian oil shale. *Int. J. Energy, Environ. Econ.* 19(4):1–16.
- Russel, P. L. 1990. *Oil Shales of the World, their Origin, Occurrence and Exploitation*. Oxford: Pergamon Press.
- Turns, Stephen R. 2000. *An Introduction to Combustion*, 2nd Boston: Ed. McGraw-Hill.